Chapter 1

# Petrology, Geochemistry and Mineralogy of Greisens Associated with Tin-Tungsten Mineralisation: Hub Stock Deposit at Krásno–Horní Slavkov Ore District, Czech Republic

Miloš René

Additional information is available at the end of the chapter

http://dx.doi.org/10.5772/intechopen.71187

**Abstract**

The greisens evolved in the apical part of the Hub stock, formed by weakly greisenised topaz granites, are predominantly represented by Li-mica-topaz and topaz-Li-mica greisens. These greisens, relative to weakly greisenised topaz granites, are enriched in Ca, F, Fe, Li, Si, Sn and W and depleted in Al, K, Mg, Na, Ti, Y, Zr and ΣREE. Weakly greisenised topaz granites show convex tetrads in the normalised REE patterns. Compared to topaz granites, the greisens display lower ΣREE concentrations, partly higher negative Eu anomaly, high Y/Ho and low Zr/Hf ratios. Li-micas occurring in greisens are represented by zinnwaldite. Chemical composition of cassiterite is near to ideal $SnO_2$ (>99 wt.% $SnO_2$). The wolframite is represented by manganoan ferberite.

**Keywords:** greisen, topaz granite, petrology, geochemistry, Li-mica, cassiterite, wolframite

## 1. Introduction

Greisenisation is one of the most significant wall rock alterations, which occurs in granite-related tin-tungsten ore deposits [1–9]. Historically, the term "greisen" has been used firstly by miners from the Krušné Hory/Erzgebirge Mts. to describe wall rocks consisting of quartz, mica and topaz surrounding the Sn-W mineralisation [10]. This area hosts a number of Sn-W deposits (e.g., Cínovec/Zinnwald, Altenberg, Ehrenfriedersdorf, Krásno–Horní Slavkov) bound to greisenised stocks of the Variscan granitic bodies. These granites represent highly fractionated granites of the Krušné Hory/Erzgebirge batholith [11–13]. Besides the Cornwall

ore fields in England, these deposits were an important European source of tin from the Bronze Age until 1991. The largest Sn-W-Li-Nb-Ta ore deposit in the Krásno–Horní Slavkov ore district is part of the Hub and Schnöd granite stocks, where Sn-W mineralisation of the greisen type was exploited from the 1200s to 1991. The total historical production of the Krásno–Horní Slavkov ore district is estimated at 52,000 tons of tin [14, 15].

This study was carried out to characterise petrological, mineralogical and geochemical features of the Hub stock greisens. The presented data provide a basis for definition of the alteration zoning and also basis for estimating the magnitude of mass transfer and the integrated fluid flux involved in the formation of the stock greisen system.

## 2. Geological setting

The Krásno–Horní Slavkov ore district comprises mineralised topaz granite stocks along the SE margin of the Krudum granite body in the Slavkovský les Mts. area (**Figure 1**). The Krudum granite body is part of the Western Erzgebirge pluton [16–20]. The inner structure of the granite stocks in the Krásno–Horní Slavkov ore district is remarkably stratified, comprising

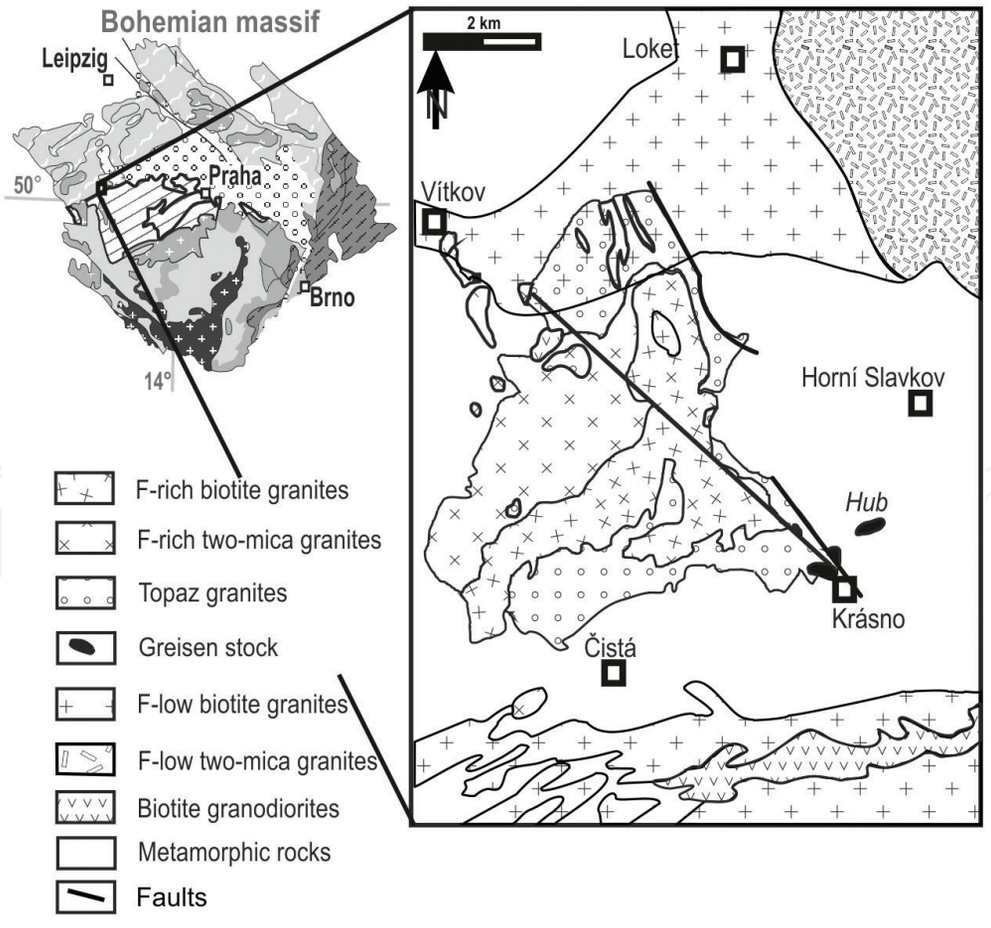


**Figure 1.** Geological sketch map of the Krásno–Horní Slavkov ore district.

greisens, weakly greisenised topaz alkali-feldspar granites, and layers of alkali-feldspar syenites (**Figure 2**). According to the most widely accepted genetic models, the topaz alkali-feldspar granite stocks represent the apical parts of highly fractionated granite bodies [12, 18, 19]. Greisens with Sn-W mineralisation are developed predominantly in the upper part of the Hub stock (**Figures 2** and **3**). The greisens are represented according to modal classification [2] predominantly by Li-mica-topaz and topaz-Li-mica greisens. The Li-mica and quartz greisens are less abundant. Very rare topaz greisens occur as small lenses in topaz-Li-mica greisens. Greisens occur in two structural types [19, 21]. The first and dominant one (greisens I) forms irregular bodies and lenses of various sizes. The uppermost part of the Hub stock is filled by massive greisen body, alternating deeper in the stock centres with weakly or intensively altered topaz granites. The lenticular greisen bodies are locally oriented parallel to the elongation of the stock; however, their form is usually irregular without sharp contact with weakly altered granites (**Figure 3**). The second type (greisen II) forms fracture-controlled bodies, sometimes occurring together with quartz veins (**Figure 4a**).

The occurrence of Sn-W mineralisation is controlled by the contact between granites and gneissic country rock. The highest ore concentrations occur, with some exceptions, in greisens and less frequently in the highly greisenised and argillitised topaz granites. The Sn-W mineralisation can be subdivided into (1) disseminated-type mineralisation, (2) ore domains, and (3) quartz veins. The disseminated mineralisation found in those greisens has typical content of 0.2–0.3 wt.% Sn. The ore domains are globular or even irregular bodies with tens

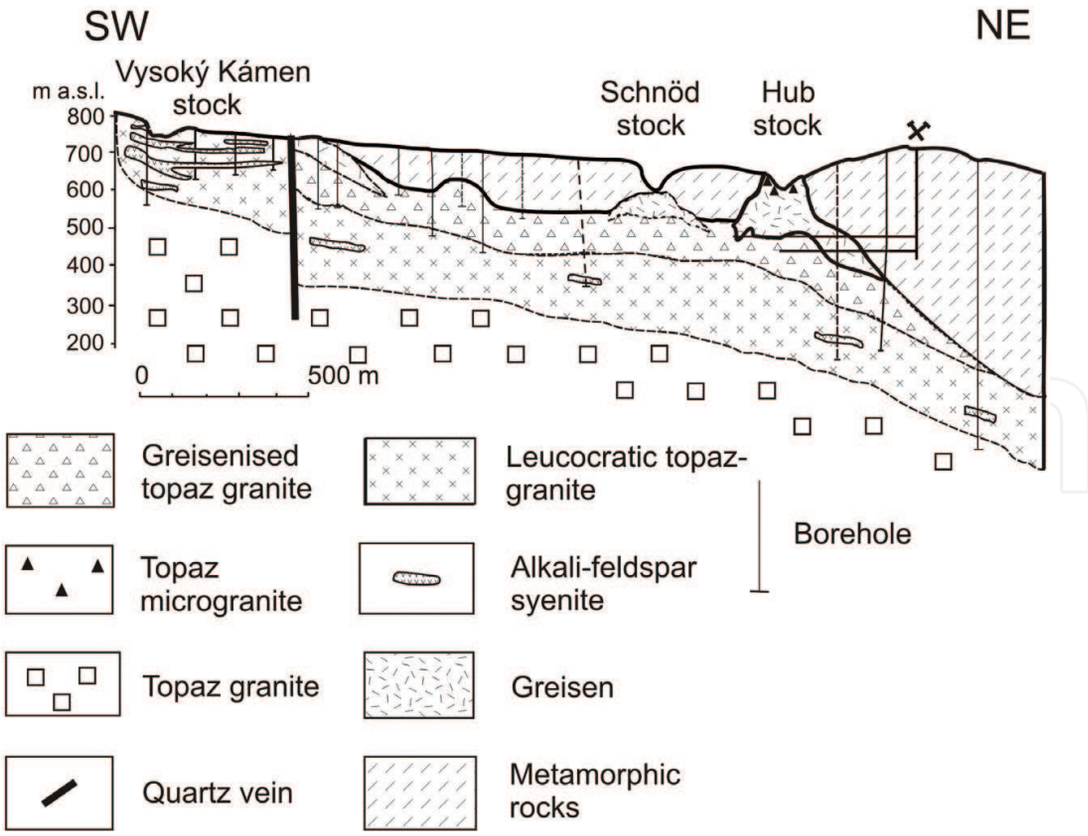


**Figure 2.** Schematic cross section of the south-eastern part of the Krudum granite body (after [19], modified by author).

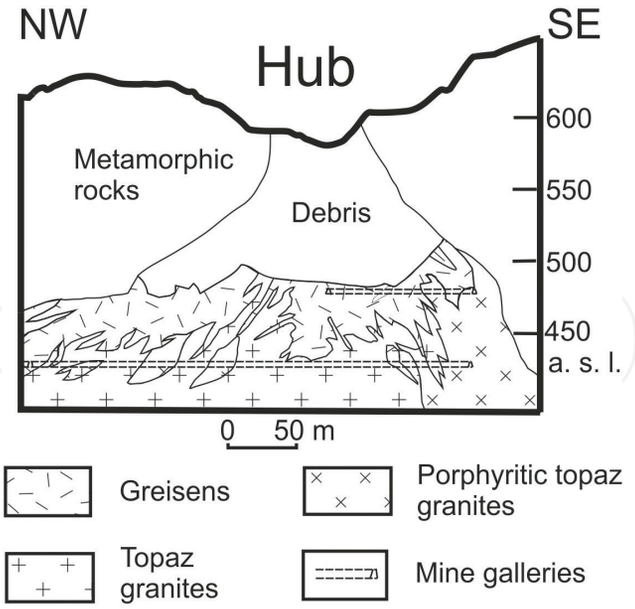


**Figure 3.** Schematic cross section of the hub stock (after [19], modified by author).

of centimetres in size, with a very high proportion of cassiterite (**Figure 4b**). Quartz, Li-mica, muscovite, and clay minerals (dickite, kaolinite, smectite and very rare cookeite and tosudite) are the accompanying minerals of these domains. Muscovite together with clay minerals forms a younger filling in vugs occurring in the ore domains [22, 23]. The NE–SW trending quartz veins are developed mainly in exocontact of the granite stock and less in greisen bodies, where they do not usually exceed 15 cm in thickness. In the uppermost part of the Hub stock occurs also quartz bodies with size more tens meters. Besides quartz, the quartz veins contain cassiterite and wolframite, sometimes Li-mica, apatite, and fluorite with highly variable amounts of Fe-Cu-As-Zn-Sn sulphides. The high enrichment in these sulphides especially in arsenopyrite and chalkopyrite occurs in the uppermost part of the Hub stock.

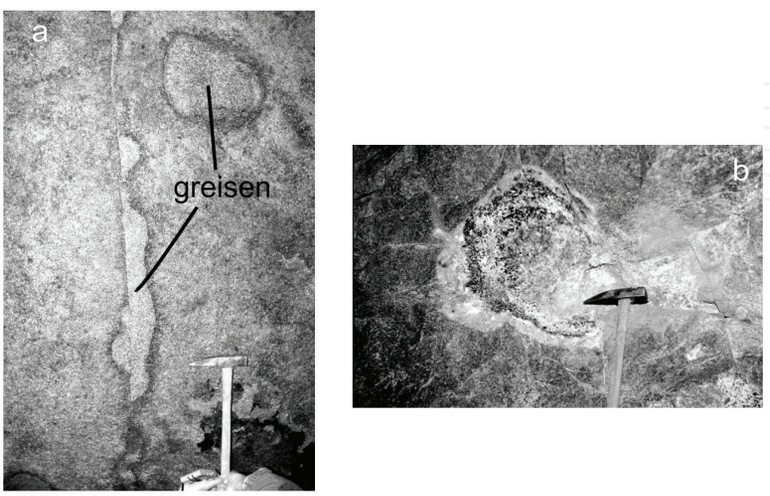


**Figure 4.** (a) Greisenisation II developed around the fissure in weakly greisenised topaz granite, hub stock, 4 level; (b) cassiterite-rich ore domain hosted in weakly greisenised topaz granite, hub stock, 4 level (photo of M. Košatka, 1987).

http://dx.doi.org/10.5772/intechopen.71187

## 3. Samples and methods

The samples used in this study include archive material from underground mine workings and from underground boreholes performed in the area of the Hub stock. The studied greisens were sampled during the last exploration phase of this ore deposit (1987–1991). Approximately, 80 greisen and 30 topaz granite samples were used for this study. Major elements and selected trace elements (Ba, Rb, Sr, Y, Zr, Nb, Ga, and Sn) were determined by X-ray fluorescence spectrometry using the Philips PW 1410 spectrometer at chemical laboratory of the DIAMO Ltd., Stráž pod Ralskem, Czech Republic. The FeO content was measured by titration, whereas the loss on ignition (LOI) was determined gravimetrically in the same laboratory. The F content was determined using an ion-selective electrode, also at chemical laboratory of the DIAMO Ltd. For selected 10 samples, the trace elements, inclusive REE, were determined by inductively coupled plasma mass spectrometry (ICP MS) using a Perkin Elmer Sciex ELAN 6100 ICP mass spectrometer at Activation Laboratories Ltd., Ancaster, Canada. The decomposition of the rock samples for ICP-MS analysis involved lithium metaborate/tetraborate fusion. Since the analytical procedure for ICP MS involves lithium metaborate/tetraborate flux fusion, the Li concentration was analysed separately by atomic absorption spectrometry on a Varian 220 spectrometer at the Analytical laboratory of the Institute of Rock Structure and Mechanics, v.v.i. (Academy of Sciences of the Czech Republic). The density of these selected samples was determined pycnometrically at the same laboratory. Approximately 55 quantitative electron-microprobe analyses of selected minerals (Li-mica, cassiterite, and wolframite) were performed using four representative polished thin sections of greisens. Minerals were analysed in polished thin sections to obtain information about mineral zoning in examined rocks. Back-scattered electron images (BSE) were acquired to study the compositional variation of individual mineral grains. The elemental abundances of Al, Ba, Ca, Cl, F, Fe, In, K, Mg, Mn, Na, Nb, P, Rb, Sc, Si, Sn, Ta, Ti, U, W, Y, and Zr were determined using a CAMECA SX 100 electron microprobe operated in wavelength-dispersive mode at the Institute of Geological Sciences, Masaryk University in Brno. The accelerating voltage and beam currents were 15 kV and 20 or 40 nA, respectively, with a beam diameter ranging from 1 to 5 μm. Peak count-time was 20 s and background time 10 s for major elements, whereas for trace elements, 40–60 s and 20–30 s, respectively, were used. The raw data were corrected using the PAP matrix corrections [24]. The detection limits were approximately 450 ppm for Nb, 720 ppm for Ta, 600–700 ppm for U, 400–500 ppm for Y, and 600 ppm for Zr. The concentration of $Li_2O$ in analysed micas was estimated using the following empirical equation [$Li_2O = (0.289 \times SiO_2) - 9.658$], recommended by Tischendorf et al. [25].

## 4. Results

### 4.1. Petrography

Weakly greisenised topaz alkali-feldspar granites (hight-F, high-$P_2O_5$ Li mica granites according to Ref. [11]) are medium-grained, equigranular rocks consisting of quartz, albite ($An_{0–2}$),

potassium feldspar, Li-mica, and topaz. Apatite, zircon, Nb-Ta-Ti oxides, xenotime-(Y), monazite-(Ce), uraninite, and coffinite are common accessory minerals. Porphyritic, weakly greisenised topaz alkali-feldspar granites occur as relatively small lenses in the main granite body of equigranular topaz granites (**Figure 3**). Their groundmass is fine-grained with phenocrysts of potassium feldspar. Granites contain quartz, albite ($An_{0–5}$), potassium feldspar, Li-mica and topaz. Apatite, zircon, Nb-Ta-Ti oxides, xenotime-(Y) and monazite-(Ce) are common accessories.

Greisens I are mostly medium-grained, equigranular rocks consisting quartz, lithium mica and topaz (**Figure 5a**). Apatite, zircon, Nb-Ta-Ti-oxides, cassiterite and wolframite are common accessory minerals. Three mineralogical types of greisens were distinguished: (1) medium grained Li-mica-topaz and topaz-Li-mica greisens which prevail contain predominantly quartz (50–75 vol.%) accompanied by equant or columnar grains of topaz (9–23 vol.%) and plates of Li-mica (15–30 vol.%); (2) medium-grained quartz greisens and Li-mica greisens occur in the upper parts of the Hub stock. They are composed of 70–95 vol.% of quartz, about 5 vol.% of subhedral topaz and 5–25 vol.% of Li-mica flakes; (3) coarse-grained topaz greisens occur very rarely as small lenses enclosed in medium-grained Li-mica-topaz greisens. These greisens are also enriched in apatite. Li-mica-topaz and topaz-Li-mica greisens were partly overprinted by younger lower temperature fluids, which is evident as lithium mica together with topaz is altered to very fine-grained aggregates of muscovite (**Figure 5b**).

### 4.2. Whole-rock chemistry

The weakly greisenised topaz alkali-feldspar granites are a highly peraluminous rocks with an aluminium saturation index (ASI = mol.% $Al_2O_3/(CaO + Na_2O + K_2O)$ ranging from 1.1 to 1.5. In comparison with common Ca-poor, S-type granites [26], they are enriched in incompatible elements such as Rb (830–1500 ppm), Cs (38–150 ppm), Sn (19–6200 ppm), Nb (18–83 ppm), Ta (8–53 ppm) and W (4–62 ppm) but poor in Mg (0.1–0.2 wt.% MgO), Ca (0.3–1.0 wt.% CaO), Sr (12–50 ppm), Ba (21–81 ppm) and Zr (20–55 ppm). Granites are distinctly enriched in P (0.3–0.4 wt.% $P_2O_5$) and F (0.1–0.8 wt.% F). A highly evolved nature is reflected in the low K/Rb value (15–47).

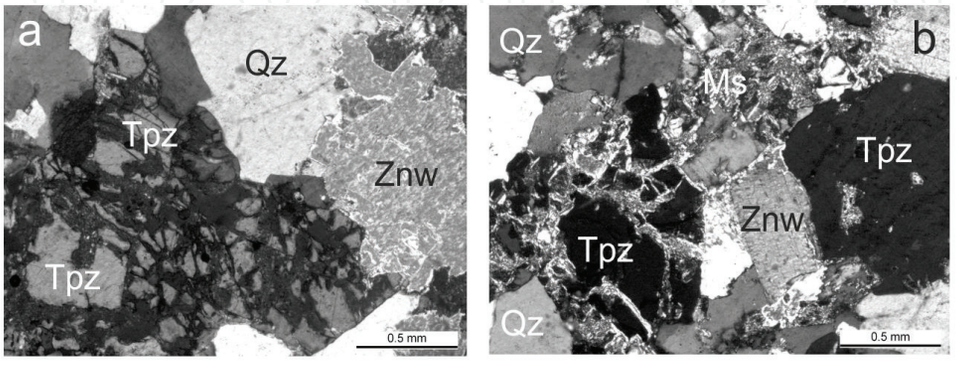


**Figure 5.** (a) Microphotographs of typical Li-mica-topaz greisens from the Hub stock. (a) Quartz-topaz aggregates with Li-mica flakes; (b) topaz and Li-mica altered by younger very fine aggregates of muscovite (photo of M. René, 2014).

http://dx.doi.org/10.5772/intechopen.71187

Li-mica-topaz and topaz-Li-mica greisens are in comparison with original topaz granites enriched in Si (up to 84.4 wt.% $SiO_2$), Fe (0.3–4.7 wt.% $FeO_{tot.}$), F (0.1–2.8 wt.% F), Rb (201–2065 ppm), Cs (120–211 ppm), Sn (23–16,300 ppm), Nb (23–409 ppm) and W (15–160 ppm) but depleted in Na (0.2–0.6 wt.% $Na_2O$) and K (1.5–4 wt.% $K_2O$) and Zr (2–33 ppm). Li-mica greisens and especially topaz greisens are enriched in Al (up to 34.6 wt.% $Al_2O_3$) and depleted in Si, K, Na, Fe and Rb (**Table 1** and **Figure 6**).

| **Sample** | **999** | **1007** | **1283** | **1285** | **1000** | **1167** | **1441** | **1457** |
|---|---|---|---|---|---|---|---|---|
| Rock type, wt.% | TG | TG | TG | TG | GR | GR | GR | GR |
| $SiO_2$ | 71.09 | 73.28 | 73.71 | 74.34 | 77.33 | 81.27 | 75.15 | 79.92 |
| $TiO_2$ | 0.09 | 0.06 | 0.04 | 0.05 | 0.03 | 0.03 | 0.03 | 0.04 |
| $Al_2O_3$ | 16.07 | 14.81 | 15.40 | 15.05 | 12.64 | 11.04 | 14.14 | 13.99 |
| $Fe_2O_3$ | 0.10 | 0.04 | 0.01 | 0.06 | 0.10 | 0.58 | 0.25 | 0.07 |
| FeO | 1.08 | 0.91 | 0.77 | 0.81 | 1.30 | 1.90 | 2.73 | 1.95 |
| MnO | 0.08 | 0.08 | 0.04 | 0.05 | 0.12 | 0.14 | 0.17 | 0.13 |
| MgO | 0.23 | 0.17 | 0.05 | 0.05 | 0.05 | 0.05 | 0.05 | 0.10 |
| CaO | 0.53 | 0.60 | 0.40 | 0.38 | 1.57 | 0.34 | 0.77 | 0.36 |
| $Na_2O$ | 3.17 | 3.25 | 3.72 | 3.49 | 0.92 | 0.20 | 0.20 | 0.20 |
| $K_2O$ | 4.85 | 4.75 | 4.12 | 3.69 | 1.41 | 1.86 | 3.06 | 1.59 |
| $P_2O_5$ | 0.33 | 0.31 | 0.27 | 0.27 | 0.44 | 0.18 | 0.27 | 0.23 |
| $H_2O^+$ | 1.80 | 1.20 | 0.05 | 0.41 | 3.40 | 0.35 | 1.46 | 0.77 |
| $H_2O^-$ | 0.00 | 0.00 | 0.00 | 0.32 | 0.00 | 0.50 | 0.42 | 0.26 |
| F | 0.76 | 0.68 | 0.12 | 0.16 | 2.00 | 1.80 | 0.56 | 0.84 |
| O = F | 0.32 | 0.29 | 0.05 | 0.07 | 0.84 | 0.76 | 0.24 | 0.35 |
| Total | 99.93 | 99.85 | 98.65 | 99.06 | 100.54 | 99.48 | 99.04 | 100.11 |
| ppm | | | | | | | | |
| Ba | 55 | 26 | 23 | 21 | 22 | 11 | 28 | 34 |
| Rb | 1320 | 1030 | 1150 | 1160 | 732 | 1040 | 1000 | 971 |
| Y | 10 | 7 | 10 | 10 | 3 | 2 | 6 | 5 |
| Zr | 39 | 37 | 53 | 40 | 28 | 20 | 21 | 16 |
| Th | 5 | 6 | 9 | 7 | 2 | 3 | 4 | 3 |
| La | 3.54 | 5.06 | 3.46 | 3.77 | 1.83 | 1.33 | 2.35 | 2.13 |
| Ce | 8.09 | 10.32 | 7.91 | 8.70 | 2.12 | 1.47 | 3.62 | 3.26 |
| Pr | 0.95 | 1.21 | 0.91 | 1.03 | 0.23 | 0.17 | 0.43 | 0.39 |
| Nd | 4.01 | 5.43 | 3.47 | 4.22 | 1.08 | 0.84 | 2.16 | 1.95 |
| Sm | 1.38 | 1.38 | 1.07 | 1.39 | 0.31 | 0.25 | 0.65 | 0.59 |

| Sample | 999 | 1007 | 1283 | 1285 | 1000 | 1167 | 1441 | 1457 |
|---|---|---|---|---|---|---|---|---|
| Eu | 0.09 | 0.14 | 0.03 | 0.08 | 0.01 | 0.01 | 0.03 | 0.01 |
| Gd | 1.46 | 1.25 | 1.09 | 1.42 | 0.23 | 0.18 | 0.60 | 0.54 |
| Tb | 0.33 | 0.24 | 0.25 | 0.30 | 0.07 | 0.04 | 0.15 | 0.12 |
| Dy | 1.85 | 1.52 | 1.67 | 1.74 | 0.42 | 0.28 | 0.99 | 0.81 |
| Ho | 0.31 | 0.28 | 0.30 | 0.31 | 0.07 | 0.05 | 0.15 | 0.13 |
| Er | 1.03 | 0.88 | 0.87 | 0.98 | 0.20 | 0.14 | 0.45 | 0.40 |
| Tm | 0.18 | 0.12 | 0.18 | 0.18 | 0.04 | 0.03 | 0.09 | 0.08 |
| Yb | 1.25 | 0.89 | 1.16 | 1.16 | 0.30 | 0.19 | 0.59 | 0.53 |
| Lu | 0.17 | 0.17 | 0.15 | 0.15 | 0.04 | 0.02 | 0.08 | 0.07 |
| $La_N/Yb_N$ | 1.91 | 3.82 | 2.02 | 2.20 | 4.12 | 4.73 | 2.69 | 2.72 |
| Eu/Eu* | 0.20 | 0.32 | 0.09 | 0.18 | 0.11 | 0.14 | 0.15 | 0.05 |

TG: weakly greisenised topaz granites, GR: topaz-Li-mica and Li-mica-topaz greisens, $Eu/Eu^* = Eu_N/\sqrt{[(Sm_N) \times (Gd_N)]}$, normalised by chondrite using normalising value according to Ref. [28].

**Table 1.** Representative whole-rock chemical analyses of weakly greisenised topaz granites and greisens from the hub stock, Krásno-Horní Slavkov ore district.

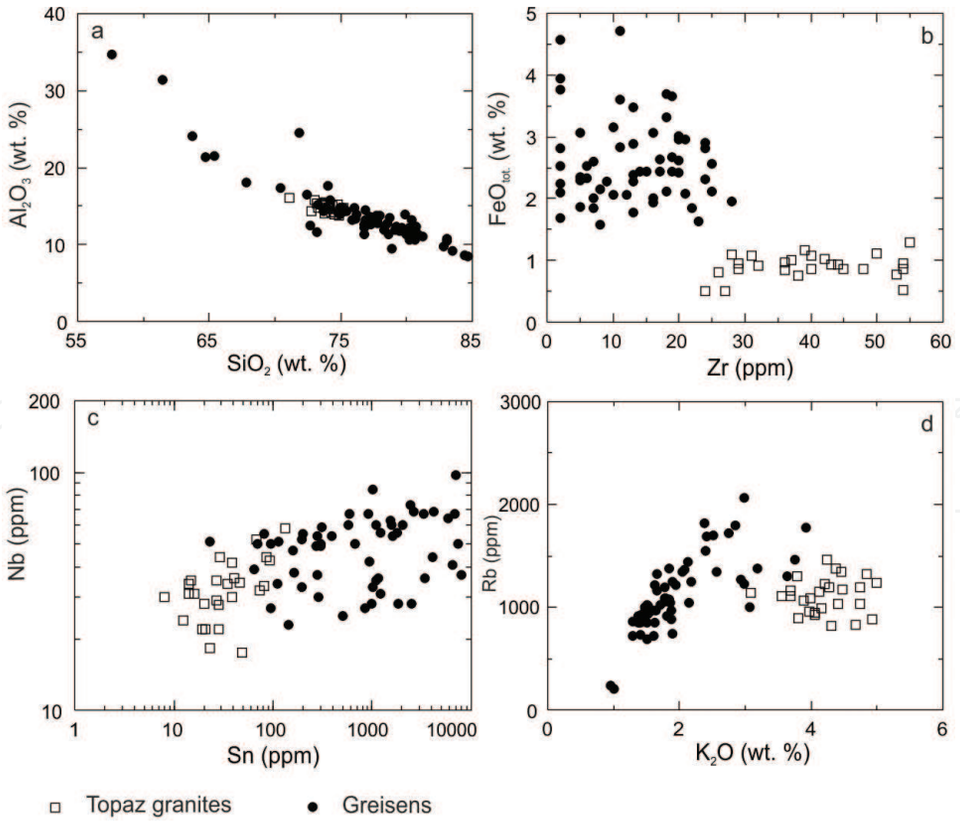


**Figure 6.** Whole-rock chemistry of the weakly greisenised topaz granites and different Li-mica-topaz greisens.

http://dx.doi.org/10.5772/intechopen.71187

The normalised REE patterns indicate the decreases in the LREE and HREE in greisens compared to weakly greisenised topaz granites and steep slopes from La to Sm but almost horizontal patterns between Gd and Lu. Both rock types show prominent negative europium anomaly. An additional feature that influences the distribution of the REEs in both rock types is the lanthanide tetrad effect. Quantification of the tetrad effect sizes was carried out using method proposed by Irber [27]. Weakly greisenised topaz granites show convex tetrads in the normalised REE patterns (**Table 2** and **Figure 7**).

| Rock type | Topaz granites (n = 15) | Greisens (n = 4) |
|---|---|---|
| Σ REE | 11.17–45.97 | 5.00–12.33 |
| $La_N/Yb_N$ | 1.62–4.81 | 2.69–4.73 |
| $La_N/Sm_N$ | 1.61–2.41 | 2.27–3.71 |
| $Eu_N/Yb_N$ | 0.02–0.51 | 0.05–0.13 |
| Eu/Eu* | 0.03–0.32 | 0.05–0.14 |
| $TE_{1–3}$ | 1.00–1.30 | 0.89–1.04 |

**Table 2.** Distribution of REE in weakly greisenised topaz granites and greisens from the Hub stock.

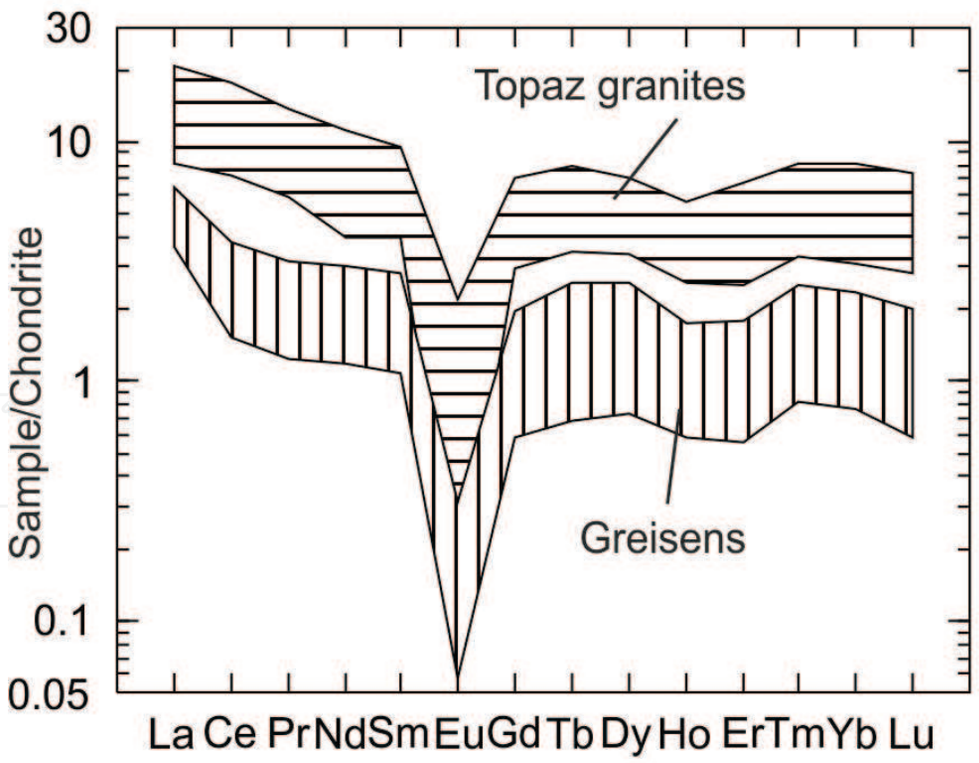


**Figure 7.** Chondrite normalised REE patterns of weakly greisenised topaz-albite granites and Li-mica-topaz greisens. Normalising values according to Ref. [28].

## 5. Mass changes during greisenisation

The origin of greisens is essentially connected to the chemical losses and gains from the alteration of the parent weakly greisenised topaz granites. For the detailed investigation of losses and gains during greisenisation, the isocon method developed by Grant [29] was applied. The scattering of the elements in the isocon plot for selected samples of Li-mica-topaz greisen suggests that the major and trace elements were mobile to variable extent (**Figure 8**). Origin of Li-mica-topaz greisen was connected with enrichment of Ca, F, Fe, Li, Mn, Si, Sn and W and loss of Al, Ba, K, Mg, Na, P, Rb Th, Y and Zr. Elements hosted by accessory zircon, monazite and xenotime (such as Zr, Th and Y) become partly depleted during greisenisation. The oxides as $K_2O$ and $Na_2O$, together with Rb and Ba, were removed due to feldspar dissolution.

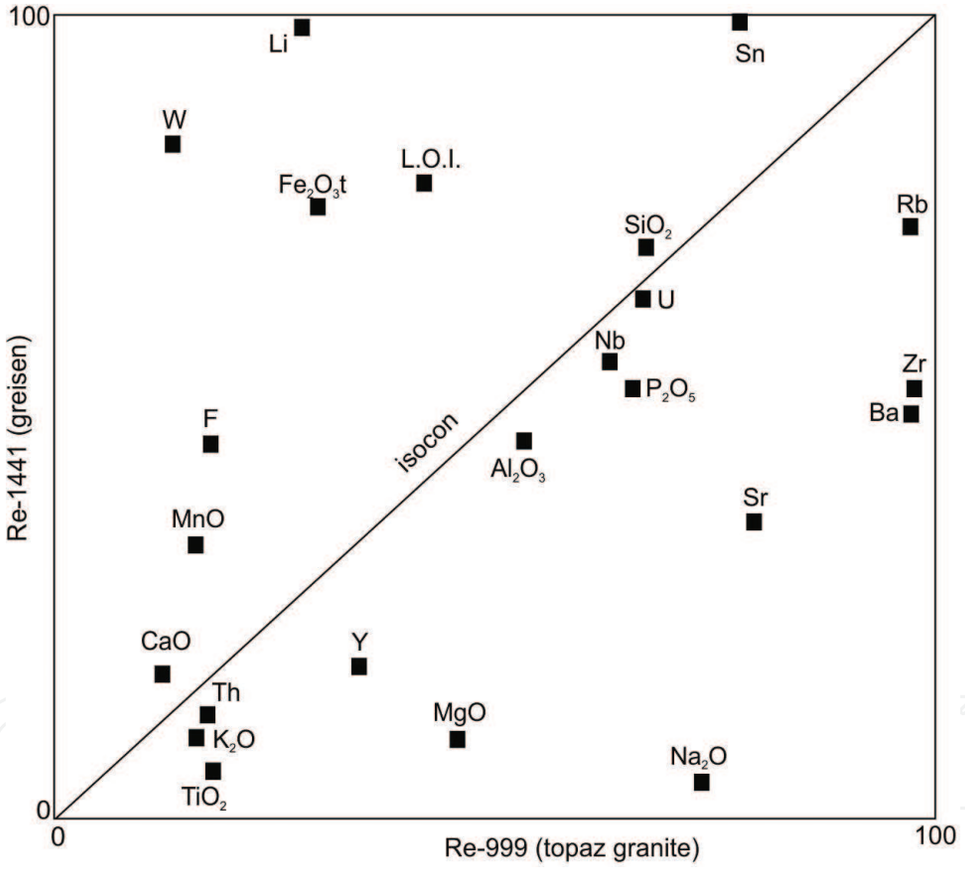


**Figure 8.** Normalised isocon plot of the Li-mica-topaz greisen (1441) vs. partly greisenised topaz granite (999).

## 6. Mineral chemistry

### 6.1. Lithian mica

Lithian mica in greisens according classification of Tischendorf et al. [25] is represented by Fe-rich polylithionite (**Figure 9** and **Table 3**). Grains of zinnwaldite are chemically homogeneous, without

http://dx.doi.org/10.5772/intechopen.71187

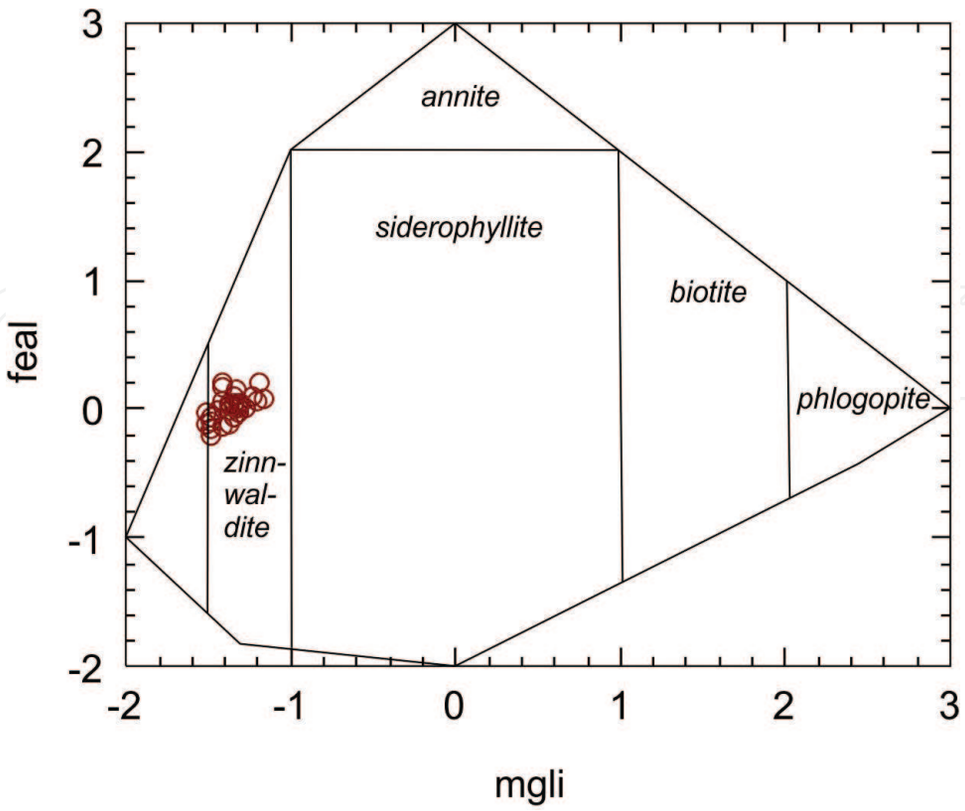


**Figure 9.** Subdivision of trioctahedral K-mica varieties in the mgli-feal diagram according to Ref. [26] with analyses of Li-mica from Li-mica-topaz greisens, Hub stock.

| Sample, wt.% | 1000-1 | 1000-3 | 1000-4 | 1000-7 | 1167-14 | 1167-16 | 1167-18 | 1167-20 |
|---|---|---|---|---|---|---|---|---|
| $SiO_2$ | 42.05 | 42.22 | 42.18 | 41.37 | 41.41 | 42.29 | 41.41 | 41.59 |
| $TiO_2$ | 0.47 | 0.18 | 0.07 | 0.27 | 0.30 | 0.05 | 0.26 | 0.45 |
| $Al_2O_3$ | 22.06 | 22.56 | 22.28 | 22.38 | 22.45 | 22.29 | 22.50 | 21.73 |
| FeO | 14.64 | 14.38 | 14.74 | 15.14 | 15.08 | 14.98 | 15.15 | 15.81 |
| MnO | 0.63 | 0.60 | 0.66 | 0.64 | 0.81 | 0.79 | 0.72 | 0.66 |
| MgO | 0.13 | 0.13 | 0.11 | 0.13 | 0.04 | 0.04 | 0.04 | 0.03 |
| BaO | b.d.l. | b.d.l. | 0.02 | 0.03 | b.d.l. | b.d.l. | 0.02 | b.d.l. |
| CaO | b.d.l. | 0.02 | b.d.l. | 0.03 | b.d.l. | b.d.l. | b.d.l. | b.d.l. |
| $Na_2O$ | 0.16 | 0.27 | 0.22 | 0.23 | 0.27 | 0.22 | 0.21 | 0.23 |
| $K_2O$ | 10.12 | 9.97 | 10.40 | 10.06 | 9.97 | 10.20 | 10.07 | 9.95 |
| $Rb_2O$ | 0.74 | 0.66 | 0.59 | 0.65 | 0.71 | 0.62 | 0.81 | 0.84 |
| $Li_2O$calc. | 2.49 | 2.54 | 2.53 | 2.30 | 2.31 | 2.56 | 2.31 | 2.36 |
| F | 5.16 | 5.31 | 5.79 | 4.98 | 5.47 | 4.83 | 5.07 | 5.01 |
| Cl | 0.01 | b.d.l. | b.d.l. | 0.02 | 0.01 | b.d.l. | 0.01 | b.d.l. |
| O = F, Cl | 2.17 | 2.24 | 2.44 | 2.10 | 2.31 | 2.03 | 2.14 | 2.11 |
| Total | 96.49 | 95.86 | 97.15 | 96.13 | 96.52 | 96.84 | 96.44 | 96.55 |

| Sample, wt.% | 1000-1 | 1000-3 | 1000-4 | 1000-7 | 1167-14 | 1167-16 | 1167-18 | 1167-20 |
|---|---|---|---|---|---|---|---|---|
| apfu, O = 22 | | | | | | | | |
| $Si^{4+}$ | 6.22 | 6.22 | 6.23 | 6.17 | 6.16 | 6.23 | 6.16 | 6.20 |
| $Al^{4+}$ | 1.78 | 1.78 | 1.77 | 1.84 | 1.84 | 1.77 | 1.84 | 1.81 |
| $Ti^{4+}$ | 0.05 | 0.02 | 0.01 | 0.03 | 0.03 | 0.01 | 0.03 | 0.05 |
| $Al^{6+}$ | 2.07 | 2.14 | 2.10 | 2.09 | 2.10 | 2.10 | 2.10 | 2.01 |
| $Fe^{2+}$ | 1.81 | 1.77 | 1.82 | 1.89 | 1.88 | 1.85 | 1.89 | 1.97 |
| Mn | 0.08 | 0.08 | 0.08 | 0.08 | 0.10 | 0.10 | 0.09 | 0.08 |
| $Mg^{2+}$ | 0.03 | 0.03 | 0.02 | 0.03 | 0.01 | 0.01 | 0.01 | 0.01 |
| $Ba^{2+}$ | 0.00 | 0.00 | 0.00 | 0.00 | 0.00 | 0.00 | 0.00 | 0.00 |
| $Ca^{2+}$ | 0.00 | 0.00 | 0.00 | 0.01 | 0.00 | 0.00 | 0.00 | 0.00 |
| $Na^{1+}$ | 0.05 | 0.08 | 0.06 | 0.07 | 0.08 | 0.06 | 0.06 | 0.07 |
| $K^{1+}$ | 1.91 | 1.87 | 1.96 | 1.91 | 1.89 | 1.92 | 1.91 | 1.89 |
| $Rb^{1+}$ | 0.07 | 0.06 | 0.06 | 0.06 | 0.07 | 0.06 | 0.08 | 0.08 |
| $Li^{1+}$ | 1.48 | 1.51 | 1.50 | 1.38 | 1.38 | 1.52 | 1.38 | 1.41 |
| $F^{1-}$ | 1.25 | 1.28 | 1.40 | 1.21 | 1.33 | 1.17 | 1.23 | 1.22 |
| $Cl^{1-}$ | 0.01 | 0.00 | 0.00 | 0.01 | 0.01 | 0.00 | 0.01 | 0.00 |
| Fe/(Fe + Mg) | 0.98 | 0.98 | 0.99 | 0.98 | 1.00 | 1.00 | 1.00 | 1.00 |

b.d.l.—below detection limit.

**Table 3.** Representative microprobe analyses and crystalochemical formulae of lithium micas from greisens, Hub stock.

internal zoning. In many places, they contain small zircon and rarely uraninite inclusions. Estimated lithium contents in analysed lithian micas from greisens reach up to 1.55 apfu (atoms per formula unit). Fluorine contents in these mica reach up to 1.40 apfu.

### 6.2. Sn-W minerals

Cassiterite occurs usually as subhedral to anhedral chemically homogenous grains in the BSE (backscatter electron) mode. Its chemical composition is near ideal $SnO_2$ (>99 wt.% $SnO_2$). The only important trace elements are Ti (up to 0.28 wt.% $TiO_2$), Fe (up to 0.16 wt.% FeO) and W (up to 0.63 wt.% $WO_3$). Contents of Ta and Nb are low, up to 0.32 wt.% $Ta_2O_5$ and up to 0.23 wt.% $Nb_2O_5$, respectively (**Table 4**).

Wolframite occurs here generally as relatively rare anhedral grains without discernible chemical zoning. The wolframite is represented by manganoan ferberite with 70–76 mol.% $FeWO_4$ (**Table 5**). Analysed wolframite is partly enriched in Nb (up to 0.72 wt.% $Nb_2O_5$ and Ta (up to 0.18 wt.% $Ta_2O_5$) with Ta/(Ta + Nb) ratios ranging from 0.11 to 0.50.

| Sample | 1167-43 | 1457-3 | 1457-4 | 1457-5 | 1457-8 | 1457-11 | 1457-12 | 1457-13 |
|---|---|---|---|---|---|---|---|---|
| $Ta_2O_5$ | 0.02 | 0.02 | b.d.l. | b.d.l. | 0.03 | 0.03 | b.d.l. | b.d.l. |
| $Nb_2O_5$ | 0.08 | 0.09 | b.d.l. | b.d.l. | 0.02 | b.d.l. | b.d.l. | b.d.l. |
| $TiO_2$ | 0.28 | 0.19 | 0.03 | 0.01 | 0.02 | 0.08 | b.d.l. | b.d.l. |
| $SnO_2$ | 99.09 | 99.51 | 99.25 | 99.00 | 99.74 | 100.04 | 99.79 | 100.13 |
| $WO_3$ | 0.05 | b.d.l. | 0.18 | 0.45 | 0.00 | 0.01 | 0.02 | 0.13 |
| FeO | 0.26 | 0.08 | 0.09 | 0.03 | 0.01 | 0.05 | 0.16 | 0.02 |
| MnO | 0.01 | 0.01 | b.d.l. | b.d.l. | 0.01 | b.d.l. | b.d.l. | 0.01 |
| Total | 99.79 | 99.89 | 99.55 | 99.49 | 99.82 | 100.19 | 99.97 | 100.28 |
| O = 2 | | | | | | | | |
| apfu | | | | | | | | |
| $Ta^{5+}$ | 0.00 | 0.00 | 0.00 | 0.00 | 0.00 | 0.00 | 0.00 | 0.00 |
| $Nb^{5+}$ | 0.00 | 0.00 | 0.00 | 0.00 | 0.00 | 0.00 | 0.00 | 0.00 |
| $Ti^{4+}$ | 0.01 | 0.00 | 0.00 | 0.00 | 0.00 | 0.00 | 0.00 | 0.00 |
| $Sn^{4+}$ | 0.99 | 0.99 | 1.00 | 1.00 | 1.00 | 1.00 | 1.00 | 1.00 |
| $W^{6+}$ | 0.00 | 0.00 | 0.00 | 0.00 | 0.00 | 0.00 | 0.00 | 0.00 |
| $Fe^{2+}$ | 0.01 | 0.00 | 0.00 | 0.00 | 0.00 | 0.00 | 0.00 | 0.00 |
| $Mn^{2+}$ | 0.00 | 0.00 | 0.00 | 0.00 | 0.00 | 0.00 | 0.00 | 0.00 |

b.d.l.—below detection limit.

**Table 4.** Representative microprobe analyses and structural formulae of cassiterite from greisens of the Hub stock (wt.%).

| Sample | 1167-28 | 1167-29 | 1167-30 | 1441-36 | 1141-37 |
|---|---|---|---|---|---|
| $WO_3$ | 75.76 | 76.22 | 76.69 | 75.98 | 75.85 |
| $Ta_2O_5$ | 0.14 | 0.15 | 0.11 | 0.10 | 0.18 |
| $Nb_2O_5$ | 0.67 | 0.72 | 0.19 | 0.04 | 0.23 |
| $SnO_2$ | 0.02 | 0.04 | b.d.l. | b.d.l. | 0.02 |
| $Bi_2O_3$ | b.d.l. | 0.04 | b.d.l. | b.d.l. | 0.03 |
| $Sc_2O_3$ | 0.01 | 0.02 | b.d.l. | 0.01 | 0.01 |
| $As_2O_3$ | b.d.l. | 0.01 | 0.01 | 0.01 | b.d.l. |
| $In_2O_3$ | b.d.l. | 0.08 | b.d.l. | 0.08 | b.d.l. |
| FeO | 16.69 | 16.88 | 16.36 | 17.29 | 17.61 |
| MnO | 6.50 | 6.39 | 6.92 | 5.59 | 5.48 |
| CaO | 0.01 | 0.02 | 0.01 | 0.02 | b.d.l. |
| Total | 99.80 | 100.61 | 99.50 | 99.12 | 99.48 |

| Sample | 1167-28 | 1167-29 | 1167-30 | 1441-36 | 1141-37 |
|---|---|---|---|---|---|
| O = 4 | | | | | |
| apfu | | | | | |
| $W^{6+}$ | 0.99 | 0.99 | 1.00 | 1.00 | 1.00 |
| $Ta^{5+}$ | 0.00 | 0.00 | 0.00 | 0.00 | 0.00 |
| $Nb^{5+}$ | 0.02 | 0.02 | 0.00 | 0.00 | 0.01 |
| $Sn^{4+}$ | 0.00 | 0.00 | 0.00 | 0.00 | 0.00 |
| $Bi^{3+}$ | 0.00 | 0.00 | 0.00 | 0.00 | 0.00 |
| $Sc^{3+}$ | 0.00 | 0.00 | 0.00 | 0.00 | 0.00 |
| $As^{3+}$ | 0.00 | 0.00 | 0.00 | 0.00 | 0.00 |
| $In^{3+}$ | 0.00 | 0.00 | 0.00 | 0.00 | 0.00 |
| $Fe^{2+}$ | 0.70 | 0.71 | 0.69 | 0.74 | 0.75 |
| $Mn^{2+}$ | 0.28 | 0.27 | 0.29 | 0.24 | 0.24 |
| $Ca^{\ddot{}2+}$ | 0.00 | 0.00 | 0.00 | 0.00 | 0.00 |

b.d.l.—below detection limit.

**Table 5.** Representative microprobe analyses and structural formulae of wolframite (wt.%).

# 7. Discussion

## 7.1. Mineral and chemical changes during greisenisation

The greisenisation is a typical hydrothermal alteration accompanying the origin of rare-metal granites and associated Sn-W-Li-Mo mineralisation [1, 7, 30–33]. Greisens of the Hub stock are formed in the uppermost part of a weakly greisenised topaz granite cupola. In a similar position occur greisen bodies in the Altenberg, Cínovec/Zinnwald, Sadisdorf and Ehrenfriedersdorf Sn-W ore deposits, representing the most significant Sn-W deposits in the Krušné Hory/Erzgebirge ore district [34].

In the Cínovec/Zinnwald granite cupola in the Eastern Erzgebirge greisen bodies consist of two structural types: (i) flat thin greisen zones and quartz veins with wall-rock greisens, (ii) irregular greisen bodies several tens of metres in size, following the morphology of the granite cupola contact [35]. Similar greisen bodies, formed in the Nejdek-Eibenstock and Horní Blatná plutons in the Western Erzgebirge, show a pattern of wall-rock alteration, the intensity of which decreases outward. All these structural types of greisen bodies display varying mineralogical composition with predominance of quartz-, topaz-, Li-mica-topaz and Li-mica greisens in the German part of the Western Erzgebirge and with predominance of quartz-, topaz-Li-mica- and Li-mica greisens in the German part of the Eastern Erzgebirge [2]. Therefore, the mineralogical compositions of greisens (I) found in the Hub stock are similar to those of the Western Erzgebirge.

http://dx.doi.org/10.5772/intechopen.71187

Chemical changes during greisenisation of topaz granites are strongly dependent on the prior state of the rock and the intensity of alteration. Silica in topaz greisens is lost, whereas in Li-mica-topaz and quartz greisens, $SiO_2$ is gained. Alumina is gained in topaz-Li-mica and in topaz greisens. Due to the decomposition of albite and alkali feldspars, there is a significant loss of Na and K. In contrast, additions of Li reflect the growth of Li-mica during greisenisation, especially in Li-mica greisens. Similar gains and losses were found in selected greisens from the German part of the Krušné Hory/Erzgebirge Mts [2].

The REE plots indicate a similar course of REE patterns in weakly greisenised topaz granite and both greisen varieties, suggesting a partial dissolution of the refractory accessory minerals, but not their complete removal. An additional feature that influences the distribution of the REE in weakly greisenised topaz granites and greisens from the Hub stock is the occurrence of the convex lanthanide tetrad effect. Older studies of the tetrad effect in fractionated granites from the Smrčiny/Fichtelgebirge and Krušné Hory/Erzgebirge Mts. proposed that processes of fluid-melt interaction caused the development of a convex tetrad effect during crystallisation of the silicate melt [27, 31]. However, more recent studies [36, 37] from the Zinnwald ore deposit in the Eastern Krušné Hory/Erzgebirge Mts. demonstrated that tetrad effect was developed prior to greisenisation in stage of sub-solidus albitisation of topaz granites. The lower ΣREE concentrations in greisens according to Ref. [37] suggested that the greisenisation resulted in remobilisation of the REEs. The depletion of the ΣREE concentrations in greisens from the Hub stock is accompanied by changes in the tetrad effect, Y/Ho, Eu/Eu* and Zr/Hf ratios (**Figure 10**). The partly increasing Y/Ho ratio in greisens could be explained by migration of fluorine-rich hydrothermal fluids [38, 39]. The more negative Eu anomaly in the greisens relative to weakly greisenised topaz granites is behaving as a divalent species during greisenisation, as predicted by Sverjensky [40] and Wood [41]. Similar increases of the negative Eu anomaly in the greisens were found in the True Hill granite greisens of southwestern New Brunswick, Canada [7]. The decreasing of Zr/Hf ratio in the greisens relative to weakly greisenised topaz granites is, according to Irber [27], affected by strong hydrothermal alteration.

### 7.2. Sn-W minerals

The Sn in cassiterite is usually substituted by Fe, Mn, Ta, Nb and W [42]. The enrichment of Ta and Nb in cassiterite is significant for those occurring in pegmatites, granites, and high-temperature quartz veins [43–45]. The cassiterite analyses from granites and pegmatites fall along a linear array with Nb + Ta and Fe + Mn—concentrations varying while mostly maintaining a ratio of 2:1 corresponding to the coupled substitution $3\ Sn^{4+} \Leftrightarrow 2(Nb, Ta)^{5+} + (Fe, Mn)^{2+}$. This relationship is common to cassiterite from highly fractionated granites and pegmatites worldwide and different to those from hydrothermal cassiterite-quartz-vein deposits and greisen deposits [44]. Although cassiterite is main ore mineral in greisens, data about Nb, Ta, and W concentrations are rare [46–50]. Cassiterites from greisens are usually distinctly depleted in Fe, Nb, and Ta in comparison to cassiterites from granites, pegmatites, and high-temperature quartz veins. This depletion is also significant for cassiterites from examined greisens. The depletion in Nb, Ta, and Fe could be explained by lower crystallisation temperature of greisen cassiterites [48].

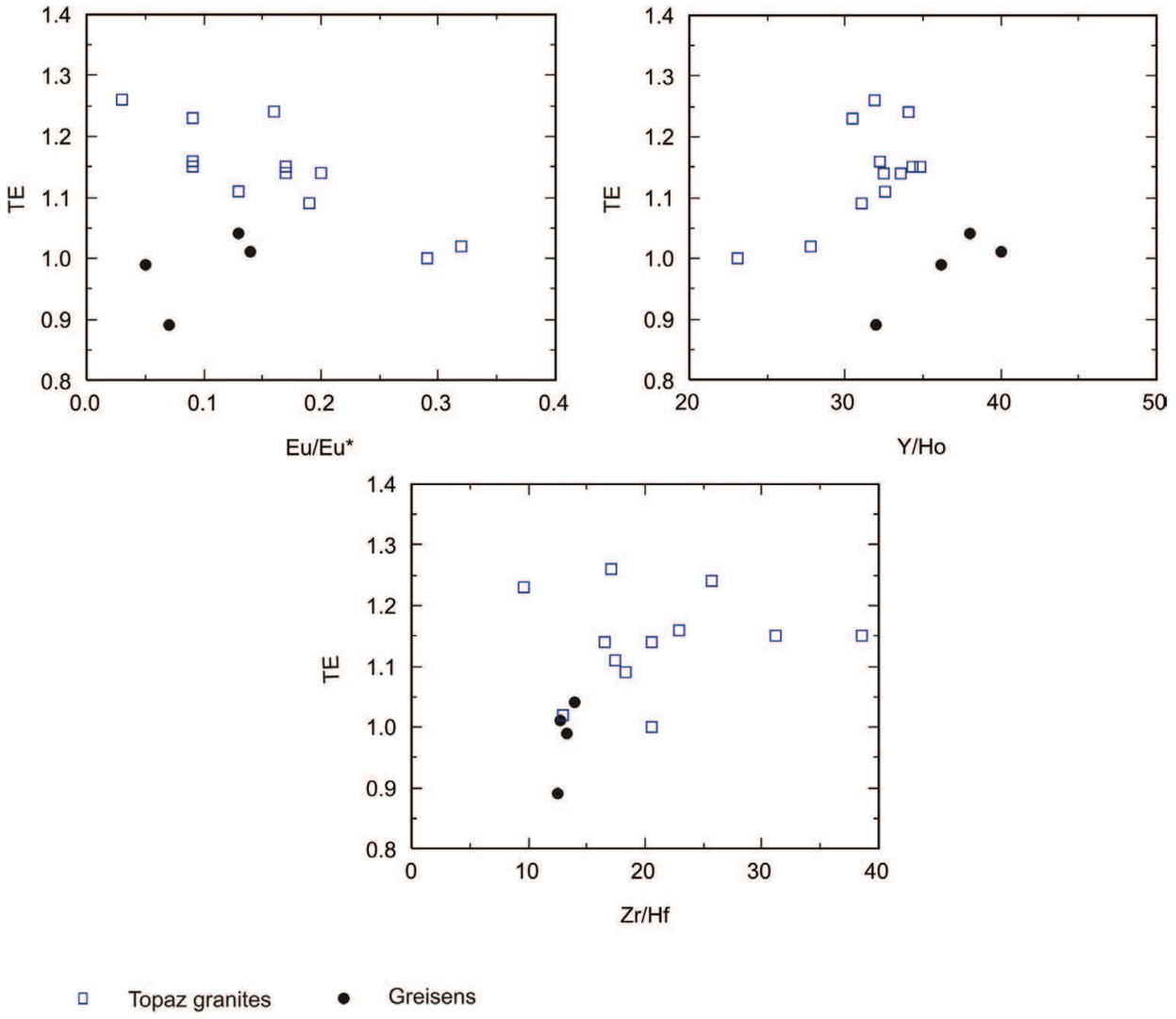


**Figure 10.** Evolution of tetrad effect, Y/Ho, Eu/Eu* and Zr/Hf ratios in the Li-mica-topaz greisens from the Hub stock.

Wolframite is solid solution between end members ferberite ($FeWO_4$) and hübnerite ($MnWO_4$) and shows a wide variety of its chemical composition. The reasons for compositional variability of Mn, Fe, and Nb in wolframite have been controversial for many years [51–56]. The empirical concept that the Mn/Fe ratios of the wolframite may vary according to the crystallisation temperature was disproved by the empirical study of wolframite and hydrothermal experiments [51, 54–57]. More recently, it was established that the wolframite compositions are determined by the compositions of the surrounding rocks, source materials, and by the Mn/Fe ratio of hydrothermal solutions [57–62]. The substitution of Nb and Ta in wolframites is supported by following substitution equation: $(Fe, Sc)^{3+} + (Nb, Ta)^{5+} \Leftrightarrow (Fe, Mn)^{2+} + W^{6+}$ [63]. The Nb and Ta are concentrated in wolframites from rare-metal granites and pegmatites, with predominance of Nb about Ta [64]. Wolframites from Sn-W deposits in the German part of the Krušné Hory/Erzgebirge ore district, including wolframites from the Hub stock, are ferberites with variable Mn/Fe ratios [65–67]. From quartz veins in the upper part of the Hub stock was also described the purest known (end-member) hübnerite. Hübnerite occurs in small cavities in these quartz veins [14].

## 8. Conclusion

The greisens of the Krásno–Horní Slavkov Ore District evolved in the apical part of the weakly greisenised topaz granite Hub stock and are represented by Li-mica-topaz, topaz-Li-mica, quartz, Li-mica and topaz greisens. These greisens occur in two structural types. The first and dominant one (greisen I) forms massive greisen bodies in the uppermost part of the Hub stock. The second type (greisen II) forms fracture-controlled bodies, sometimes occurring together with quartz veins. The disseminated Sn-W mineralisation occurring in greisens has typical content of 0.2–0.3 wt.% Sn. The predominately Li-mica-topaz and topaz-Li mica greisens relative to weakly greisenised topaz granites are enriched in Si, F, Fe, Li, Si, Sn and W and depleted in Al, K, Mg, Na, Ti, Th, Y, Zr and ΣREE. Weakly greisenised topaz granites show convex tetrads in the normalised REE patterns. The greisens display lower ΣREE concentrations, high negative Eu anomaly, high Y/Ho, and low Zr/Hf ratios relative to the topaz granites. Li-micas occurring in greisens are represented by zinnwaldite. The chemical composition of cassiterite is near ideal $SnO_2$ (>99 wt.% $SnO_2$). The wolframite is represented by manganoan ferberite with 70–76 mol.% $FeWO_4$.

## Acknowledgements

This work was carried out thanks to the support of the long-term conceptual development research organisation RVO: 67985891. The microprobe analyses were performed thanks to the financial support of the Czech Science Foundation (project No. 205/09/0540). I am grateful to R. Škoda, Š. Benedová and P. Gadas from the Institute of Geological Sciences of the Masaryk University (Brno) for technical assistance with microprobe analysis of selected minerals. I wish also to thank A. Szameitat for her constructive remarks and English corrections and book editor A. I. Al-Juboury for his very useful remarks and recommendations.

## Author details

Miloš René

Address all correspondence to: rene@irsm.cas.cz

Institute of Rock Structure and Mechanics, v.v.i., Academy of Sciences of the Czech Republic, Prague, Czech Republic

## References

[1] Rundquist DV, Denisenko VK, Pavlova IG. Greisen Deposits: Ontogenesis, Phylogenesis. Moscow: Nedra Press; 1971. 328 p (in Russian)

[2] Kühne R, Wasternack J, Schulze H. Postmagmatische Metasomatose im Endo-Exokontakt des jüngeren postkinematischen Granite des Erzgebirges. Geologie. 1972;**21**:494-520

[3] Štemprok M. Greisenization (a review). Geologische Rundschau. 1987;**76**:169-175. DOI: 10.1007/BF01820580

[4] Richardson JM, Bell K, Watkinson DH, Blenkinsop J. Genesis and fluid evolution of the east Kemptville greisen-hosted tin mine, southwestern Nova Scotia, Canada. In: Stein HJ, Hannah JL, editors. Ore-Bearing Granite Systems; Petrogenesis and Mineralizing Processes. Geol. Soc. Amer. Spec. Pap. Vol. 246. 1990. p. 181-203

[5] Schwarz MO, Surjono A. Greisenization and albitization at the Tikus tin–tungsten deposit, Belitung, Indonesia. Economic Geology. 1990;**85**:691-713. DOI: 10.2113/gsecongeo.85.4.691

[6] Pirajno F. Hydrothermal Mineral Deposits. 6th ed. New York: Springer Verlag; 1992. 732 p

[7] Lentz DR, Gregoire C. Petrology and mass. Balance constraints on major-, trace-, and rare-earth-element mobility in porphyry-greisen alteration associated with the epizonal True Hill granite, southwestern New Brunswick, Canada. Journal of Geochemical Exploration. 1995;**52**:303-331. DOI: 10.1016/0375-6742(94)00059-K

[8] Zharikov VA, Rusinov VI, Marakushev AA. Metasomatism and Metasomatic Rocks. Nauchnyi Mir: Moscow; 1998. 492 p (in Russian)

[9] Somarin AK, Ashley P. Hydrothermal alteration and mineralisation of the Glen Eden Mo-W-Sn- deposit: A leucogranite-related hydrothermal system, southern New England Orogen, NSW, Australia. Mineralium Deposita. 2004;**39**:282-300. DOI: 10.1007/s00126-003-0399-3

[10] Lempe JF. Beschreibung des Bergbaues aus dem Sächsischen Zinnwalde. Mag. Bergbaukunde. 1785:1

[11] Förster H-J, Tischendorf G, Trumbull RB, Gottesmann B. Late-collisional granites in the Variscan Erzgebirge, Germany. Journal of Petrology. 1999;**40**:1613-1645. DOI: 10.1093/petroj/40.11.1613

[12] Breiter K. Nearly contemporaneous evolution of the A- and S-type fractionated granites in the Krušné hory/Erzgebirge Mts., Central Europe. Lithos. 2012;**151**:105-121. DOI: 10.1016/j.lithos.2011.09.022

[13] Štemprok M, Blecha V. Variscan Sn-W-Mo metallogeny in gravity picture of the Krušné hory/Erzgebirge granite batholith (Central Europe). Ore Geology Reviews. 2015;**69**:285-300. DOI: 10.1016/oregeorev.2015.02.014

[14] Beran P, Sejkora J. The Krásno Sn-W ore district near Horní Slavkov: Mining history, geological and mineralogical characteristics. Journal of the Czech Geological Society. 2006;**51**:3-42

[15] Beran P, Jangl L, Majer J, Suček P, Wagenbreuth O. 1000 Years of Tin Mining in the Slavkovský les Mts. Sokolov: Okresní muzeum Sokolov; 1996. 195p (in Czech)

[16] Fiala F. Granitoids of the Slavkovský (Císařský) les Mountains. Sbor. geol. Věd G. 1968; **14**:93-160

[17] René M. Development of topaz-bearing granites of the Krudum massif (Karlovy Vary pluton). Acta Universitatis Carolinae Geologica. 1998;**42**:103-109

[18] Breiter K, Förster H-J, Seltmann R. Variscan silicic magmatism and related tin-tungsten mineralization in the Erzgebirge-Slavkovský les metallogenic province. Mineralium Deposita. 1999;**34**:505-521. DOI: 10.1007/s001260050217

[19] Jarchovský T. The nature and genesis of greisen stocks at Krásno, Slavkovský les area - western bohemia, Czech Republic. Journal of the Czech Geological Society. 2006;**51**:201-216

[20] Machek M, Roxerová Z, Janoušek V, Petrovský E, René M. Petrophysical and geochemical constraints on alteration processes in granites. Studia Geophysica et Geodaetica. 2013;**57**:710-740. DOI: 10.1007/s11200-013-0923-6

[21] Košatka M. Geological Evolution of the Hub Stock, Central Part on the Krásno Ore Deposit [Thesis]. Prague: Charles University; 1988 (in Czech)

[22] Melka K, Košatka M, Zoubková J. The occurrence of dioactahedral chlorite in greisen. In: Proceedings of the 7th Euroclay Conference; Dresden. 1991. p. 757-760

[23] Štastný M, René M. Argillization of topaz-bearing granites in the hub stock, Horní Slavkov-Krásno Sn-W ore district (bohemian massif, Czech Republic). Acta Geodynamics et Geomaterialia. 2014;**11**:255-267. DOI: 10.13168/AGG.2014.0008

[24] Pouchou JL, Pichoir F. "PAP" ($\phi$-$\varrho$-Z) procedure for improved quantitative microanalysis. In: Armstrong JT, editor. Microbeam Analysis. San Francisco: San Francisco Press; 1985. p. 104-106

[25] Tischendorf G, Rieder M, Förster H-J, Gottesmann B, Guidotti CV. A new graphical presentation and subdivision of potassium micas. Mineralogical Magazine. 2004;**68**:649-667. DOI: 10.1180/0026461046840210

[26] Chappell BW, Hine R. The Cornubian batholith: An example of magmatic fractionation on a crustal scale. Resource Geology. 2006;**56**:203-244. DOI: 10.1111/j.1751-3928.2006.tb00281.x

[27] Irber W. The lanthanide tetrad effect and its correlation with K/Rb, Eu/Eu*, Sr/Eu, Y/Ho and Zr/Hf of evolving peraluminous granite suites. Geochimica et Cosmochimica Acta. 1998;**63**:489-508. DOI: 10.1016/s0016-7037(99)0027-7

[28] Boynton WV. Geochemistry of the rare earth elements: Meteorite studies. In: Henderson P, editor. Rare Earth Element Geochemistry. Vol. 1984. Amsterdam: Elsevier; 1984. p. 63-114

[29] Grant JA. The isocon diagram–a simple solution to Gresens equation for metasomatic alteration. Economic Geology. 1986;**81**:1976-1982. DOI: 10.2113/gsecongeo.81.8.1976

[30] Wright JH, Kwak TAP. Tin-bearing greisens of mount Bischoff, northwestern Tasmania, Australia. Economic Geology. 1989;**84**:551-574. DOI: 10.2113/gsecongeo.84.3.575

[31] Halter WE, Willliams-Jones AE, Kontak DJ. The role of greisenization in cassiterite precipitation at the east Kemptville tin deposit, Nova Scotia. Economic Geology. 1996;**91**:368-385. DOI: 10.2113/gsecongeo.91.2.368

[32] Dolejš D, Štemprok M. Magmatic and hydrothermal evolution of Li-F granites: Cínovec and Krásno intrusions, Krušné hory batholith, Czech Republic. Bulletin of the Czech Geological Survey. 2001;**76**:77-99

[33] Štemprok M, Dolejš D. Fluid focusing, mass transfer and origin of fracture-controlled greisens in the Western Krušné hory granite pluton, Central Europe. Zt. Geol. Wiss. 2010;**38**:207-234

[34] Schust F. On the importance of granite elevations in the localization of greisen bodies in the Erzgebirge (Mts.). In: Fedak J, editor. The Current Metallogenic Problems of Central Europe. Vol. 1976. Warsaw: Wydawnictwa Geologiczne; 1976. p. 189-206

[35] Štemprok M, Novák JK, David J. The association between granites and tin-tungsten mineralization in the eastern Krušné hory (Erzgebirge), Czech Republic. In: von Gehlen K, Klemm DD, editors. Mineral Deposits of the Erzgebirge/Krušné Hory (Germany/Czech Republic). Berlin: Gebrüder Borntraeger; 1994. p. 97-129

[36] Monecke T, Dulski P, Kempe U. Origin of convex tetrads in rare element patterns of hydrothermally altered siliceous igneous rocks from Zinnwald Sn-W deposit, Germany. Geochimica et Cosmochimica Acta. 2007;**71**:335-353. DOI: 10.1016/j.gca.2006.09.010

[37] Monecke T, Kempe U, Monecke J, Sala M, Wolf D. Tetrad effect in rare element distribution patterns: A method of quantification with application to rock and mineral samples from granite-relalted rare metal deposits. Geochimica et Cosmochimica Acta. 2002, 2002;**66**:1185-1196. DOI: 10.1016/s0016-7037(01)00849-3

[38] Bau M, Dulski P. Comparative study of yttrium and rare-earth element behaviours in fluorine-rich hydrothermal fluids. Contributions to Mineralogy and Petrology. 1995;**119**:213-223. DOI: 10.1007/BF00307282

[39] Bau M. Controls on the fractionation of isovalent trace elements, in magmatic and aqueous systems: Evidence from Y/Ho, Zr/Hf, and lanthanide tetrad effect. Contributions to Mineralogy and Petrology. 1996;**123**:323-333. DOI: 10.1007/s004100050159

[40] Sverjensky DA. Europium redox equilibria in aqueous solution. Earth and Planetary Science Letters. 1984;**67**:70-78. DOI: 10.1016/0012-821X(84)90039-6

[41] Wood SA. The aqueous geochemistry of the rare-earth elements and yttrium. Part 2. Theoretical predictions of speciation in hydrothermal solutions to 350°C at saturated water vapor pressure. Chemical Geology. 1990;**88**:99-125. DOI: 10.1016/0009-2541(90)90106-H

[42] Möller P, Dulski P, Szacki W, Malow G, Riedel E. Substitution of tin in cassiterite by tantalum, niobium, tungsten, iron and manganese. Geochimica et Cosmochimica Acta. 1988;**52**:1497-1503. DOI: 10.1016/0016-7037(88)90220-7

[43] Murciego A, Garcia Sanchez A, Dusausoy Y, Martin Pozas JM, Ruck R. Geochemistry and EPR of cassiterites from the Iberian Hercynian massif. Mineralogical Magazine. 1997; **61**:357-365

[44] Tindle AG, Breaks FW. Oxide minerals of the separation rapids rare-element granitic pegmatite group, northwestern Ontario. The Canadian Mineralogist. 1998;**36**:609-635

[45] Abdalla HM, Matsueda H, Obeid MA, Takahashi R. Chemistry of cassiterite in rare metal granitoids and associated rocks in the Eastern Desert, Egypt. Journal of Mineralogical and Petrological Sciences. 2008, 2008;**103**:318-326. DOI: 10.2465/jmps.070528a

[46] Oen IS, Korpershoek HR, Kieft C, Lustenhouwer WJ. A microprobe study of rutile, cassiterite and wolframite and sulfides in the Morro Potosí greisen, Rondonia, Brazil. neues jahrbuch für mineralogie monatshefte. 1982;**4**:175-191

[47] Binde G. Beitrag zur Mineralogie, Geochemie und Genese des Kassiterits. Freiberg. Forsch.-H. 1986;**C411**:1-60

[48] Haapala I. Magmatic and postmagmatic processes in tin-mineralized granites: Topaz-bearing leucogranite in the Eurajoki Rapakivi granite stock, Finland. Journal of Petrology. 1997;**38**:1645-1659. DOI: 10.1093/petroj/38.12.1645

[49] Sala M. Geochemische und mineralogische Untersuchungen an alterierten Gesteinen aus dem Kuppelbereich der Lagerstätte Zinnwald (Osterzgebirge) [thesis]. Freiberg: University of Freiberg; 1999

[50] Somarin AK. Ore mineralogy and mineral chemistry of the Glen Eden Mo-W-Sn greisen-breccia system, eastern Australia. Journal of Mineralogical and Petrological Sciences. 2009;**104**:339-355. DOI: 10.2465/jmps.070929

[51] Leutwein F. Die Wolframit Gruppe. Freiberger Forschungshefte. 1951;**C8**:8-19

[52] Schröcke H. Isomorphiebeziehungen in der Wolframitgruppe. Beiträge zur Mineralogie und Petrographie. 1960;**7**:166-206

[53] Schröcke H. Heterotype Mischbarkeit zwischen Wolframit- und Columbitgruppe. Beiträge zur Mineralogie und Petrographie. 1961;**8**:92-110

[54] Taylor RG, Hosking KFG. Manganese-iron ratios in wolframite, south Crofty Mine, Cornwall. Economic Geology. 1970;**65**:47-53. DOI: 10.2113/gsecongeo/65.1.47

[55] Moore F, Howie RA. On the application of the hübnerite:Ferberite ratio as geothermometer. Mineralium Deposita. 1978;**13**:391-397. DOI: 10.1007/BF00206572

[56] Willgallis A. Zur Mischkristallverhältnis von Wolframiten. Neues Jahrbuch für Mineralogie Abhandlungen. 1982;**145**:308-326

[57] Hsu LC. The stability relations of the wolframite series. American Mineralogist. 1976; **61**:944-955

[58] Barabanov VF. Geochemistry of tungsten. International Geology Review. 1971;**13**(3):332. DOI: 10.1080/00206817109475439

[59] Groves DI, Baker WE. The regional variation in composition of wolframites from Tasmania. Economic Geology. 1972;**67**:362-368. DOI: 10.2113/gsecongeo.67.3.362

[60] Amossé J. Variations in wolframite composition according to temperature, at Borralha, Portugal, and Enguyales, France. Economic Geology. 1978;**73**:1170-1175. DOI: 10.2113/gsecongeo.73.6.1170

[61] Nakashima K, Watanabe M, Soeda A. Regional and local variations in the composition of the wolframite series from SW Japan and possible factors controlling compositional variations. Mineralium Deposita. 1986;**21**:200-206. DOI: 10.1007/BF00199801

[62] Campbell A, Petersen U. Chemical zoning in wolframite from San Cristobal, Peru. Mineralium Deposita. 1988;**23**:132-137. DOI: 10.1007/BF00206662

[63] Černý P, Ercit TS. Mineralogy of niobium and tantalum: Crystal chemical relationships, paragenetic aspects and their economic implications. In: Möller P, Černý P, Saupé F, editors. Lanthanides, Tantalum and Niobium. Berlin: Springer Verlag; 1989. p. 28-79

[64] Tindle AG, Webb PC. Niobian wolframite from Glen Gairn in the eastern highlands of Scotland: A microprobe investigation. Geochimica et Cosmochimica Acta. 1989;**53**:1921-1935. DOI: 10.1016/0016-7037(89)90313-X

[65] Kempe U, Wolf D. Die Interpretation des H/F-Koeffizienten – immer noch offen. Freiberg. Forsch.-H. 1994;**C451**:53-87

[66] Hösel G, Hoth K, Jung D, Leonhardt D, Mann M, Meyer H, Tägl U. Das Zinnerz-Lagerstättengebiet Ehrenfriedersdorf/Erzgebirge. Bergbau in Sachsen. 1994;**1**:1-196

[67] Weinhold G. Die Zinnerz-Lagerstätte Altenberg (Osterzgebirge). Bergbau in Sachsen. 2002;**9**:1-73